AIP Advances

On the prospect of CZTSSe-based thin film solar cells for indoor photovoltaic applications: A simulation study

Cite as: AIP Advances **9**, 055326 (2019); https://doi.org/10.1063/1.5099274
Submitted: 08 April 2019 . Accepted: 14 May 2019 . Published Online: 28 May 2019

K. A. Haque, and Md Zunaid Baten

AIP Publishing

On the prospect of CZTSSe-based thin film solar cells for indoor photovoltaic applications: A simulation study

Cite as: AIP Advances 9, 055326 (2019); doi: 10.1063/1.5099274
Submitted: 8 April 2019 • Accepted: 14 May 2019 •
Published Online: 28 May 2019

K. A. Haque and Md Zunaid Baten[a)]

AFFILIATIONS

Department of Electrical and Electronic Engineering, Bangladesh University of Engineering and Technology, Dhaka 1000, Bangladesh

[a)]Email: mdzunaid@eee.buet.ac.bd

ABSTRACT

In this work we present the first systematic study on the prospect of $Cu_2ZnSn(S,Se)_4$ or CZTSSe-based thin film photovoltaic devices for indoor energy harvesting applications. Based on numerical analysis, we estimate the performance characteristics of the experimentally reported highest-efficiency CZTSSe device when it is operated under a commercially available white light emitting diode (LED). The obtained efficiency of 13.77% and fill factor of 71.05% are both higher than the values reported under AM1.5 solar radiation. The results of our analysis indicate that performance enhancement under indoor condition arises from the enhanced short-circuit current at high intensity and open-circuit voltage at low intensity, which are both related to the high photon yield of the indoor spectrum corresponding to the bandgap of CZTSSe. Further performance enhancement under indoor condition can be achieved using a type-II band alignment, which we have designed and analyzed employing an intrinsic ZnO layer. The enhanced charge separation resulting from built-in-field of the ZnO layer increases the open circuit voltage by as much as 0.17 V, which in effect leads to an overall efficiency of 15.85% when operated under the considered white LED spectrum.

I. INTRODUCTION

The smooth functioning of cyber-physical systems largely rely on the operation of wired or wireless communication nodes, sensors, actuators or on-chip computers, many of which operate with only several milliwatts to few tens of micro-watts of power density.[1] Conventionally these devices are operated with batteries or grid-connected adapters, which have both limited lifetime and non-renewable sources of energy supply. Indoor photovoltaics offer a paradigm shift in how these low-power electronic devices can be supplied energy with. Particularly with recent advancements in solid-state indoor lighting systems, the technology of ambient light to electricity generation is being considered as a viable means to fulfill the energy requirement of the ever-expanding network of Internet of Things.[2–5]

Whereas the operation of outdoor photovoltaic devices is generally governed by outdoor weather and solar irradiation conditions, indoor photovoltaic (PV) devices are designed to operate under the more reliable and controllable indoor light spectrum. Moreover the maximum efficiency limit of a single-junction PV device can theoretically exceed 60% under indoor condition, which is significantly higher than the Schokley-Quisser limit of an equivalent solar cell.[3,6,7] These inherent advantages have led to the investigation of indoor PV devices employing different thin-film material systems, which include GaAs, silicon, CdTe, GaInP, perovskites, organics and dye sensitized materials.[8–12] However a material yet to be investigated in this regard is the mixed chalcogenide in the form of $Cu_2ZnSn(S,Se)_4$ or CZTSSe, which is deemed to be particularly prospective for low-cost renewable energy solutions because of the abundance of its constituent elements in the earth.[13] Moreover, the maximum theoretical efficiency predicted for CZTSSe solar cell is 32.6%, which is very close to the highest value of the Shockley-Quisser limit.[3]

In this study, we theoretically investigate the performance characteristics of kesterite-type CSTSSe PV devices under an experimentally characterized white light emitting diode (LED). By numerical simulation, we first analyze and model previously reported experimental results of the highest-efficiency CZTSSe solar cell.[18] The model is then applied to analyze the performance characteristics of the device under the measured white LED spectrum. A maximum efficiency of 13.62% is obtained under this condition, which is higher than previously reported efficiencies of CZTSSe solar cells.[14] The underlying reasons behind the higher efficiency under indoor lighting condition are investigated and a design of a CZTSSe PV device of higher efficiency is proposed and analyzed for indoor applications. It is observed that by engineering the heterostructure, efficiency of a practical CZTSSe PV device can be extended up to 15.85%, which is higher than the highest reported efficiency of a chalcogenide-based PV device operated under indoor conditions.[7,15–17]

II. PERFORMANCE COMPARISON UNDER INDOOR AND OUTDOOR CONDITIONS

The indoor light source considered in this study is a commercially available 15W, 497 lumen white LED, which is measured to have a color rendering index of 75.74% and correlated color temperature of 6175K. The measured LED spectrum along with AM1.5 solar spectrum is shown in Fig. 1(a). In order to study performance characteristics of a CZTSSe device under these spectra, a theoretical model based on numerical solution of Poisson's equation and continuity equation under optical generation-recombination conditions is considered.[19] The model is validated against output characteristics of the highest efficiency CZTSSe solar cell, the current density vs. voltage (J-V) characteristics of which is shown along with numerical calculations in Fig. 1(b). Next the theoretical model is applied to evaluate output characteristics of this device (labeled as Device A in Table I) under indoor lighting condition. Efficiency and fill factor of Device A, calculated as a function of radiation intensity (Fig. 2(a)), indicate that at all intensity levels, the device performs better under indoor conditions. For a comparative assessment, relative enhancement of fill factor (ΔFF), short circuit current density (ΔJ_{sc}), open circuit voltage (ΔV_{oc}) and overall efficiency (Δη) - each calculated with respect to the corresponding values obtained under solar radiation - are plotted in Fig. 2(b). As can be seen, the relative enhancement for short circuit current density is about twice of the values obtained for ΔV_{oc} and ΔFF at intensities above 150Wm^{-2}. However for lower intensities, the efficiency enhancement is dominated by the relative increase of the open circuit voltage, ΔV_{oc}. The maximum enhancement of overall efficiency under this condition is 14%. This is promising for the operation of this device under low-lighting conditions, which are more likely to appear under usual indoor illuminations.[2,3]

TABLE I. Different layers of the CZTSSe PV devices considered in this study.

Layers	Device A	Device B
Top Contact	Ni-Al	Ni-Al
Layer 1	n-ITO (50 nm)	n-ZnO (10 nm)
Layer 2	n-ZnO (10 nm)	i-ZnO (50 nm)
Layer 3	n-CdS (25 nm)	n-CdS (60 nm)
Layer 4	p-CZTSSe (2 um)	p-CZTSSe (2 um)
Bottom Contact	Mo	Mo

To investigate the reason behind the enhancement of the short circuit current density and open circuit voltage under indoor conditions, the photon yield of both white LED and solar spectrum are calculated and shown in Fig. 3(a). As can be observed, for the considered white LED spectrum, a photon yield of ~100% is obtained over the bandgap range of 1-1.5 eV of CZTSSe, whereas for solar irradiation this value ranges from 60-75%. Because of these high photon yields, enhancement of both J_{sc} and V_{oc} are obtained at all intensities under indoor condition. This enhancement however is limited by the device's external quantum efficiency (EQE) profile (Fig. 3(b)), which peaks at ~2.5eV under both indoor and outdoor conditions. Because the photon yields for solar and indoor radiations are rather comparable at this energy, the overall efficiency enhancement is relatively low. It is expected that the efficiency of the device can be significantly enhanced by employing an indoor spectrum which results in higher photon yield around the peak energy of the quantum efficiency profile. To further investigate operation under indoor condition, the spectral response of the device under both indoor and outdoor conditions are calculated. As shown in Fig. 3(c), spectral response of the device under indoor condition increases significantly for photon energies above 3.5eV, which is indicative of the better performance characteristics of this device in the short wavelength regime. This is further supported by the calculated carrier generation profile shown in Fig. 3(d), which indicates that generation rate in the vicinity of the p-n junction is higher

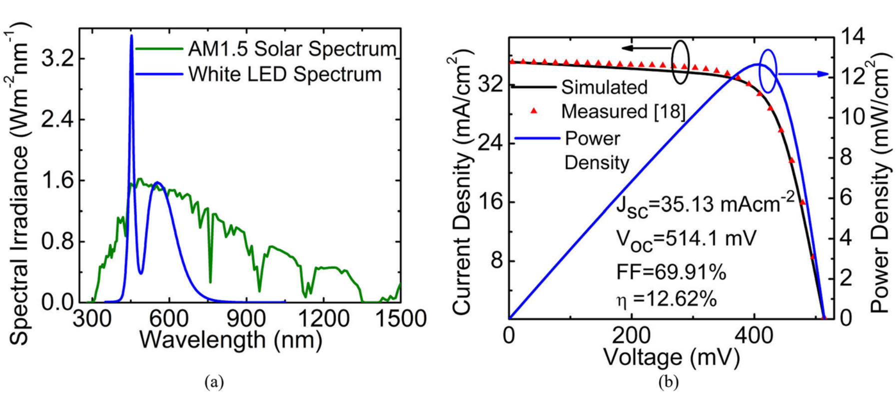

FIG. 1. (a) Measured white LED spectrum along with the considered ASTMG173 AM1.5 solar spectrum; (b) theoretically calculated current density vs. voltage and power density vs. voltage relations along with experimentally measured values reported in Ref. 18.

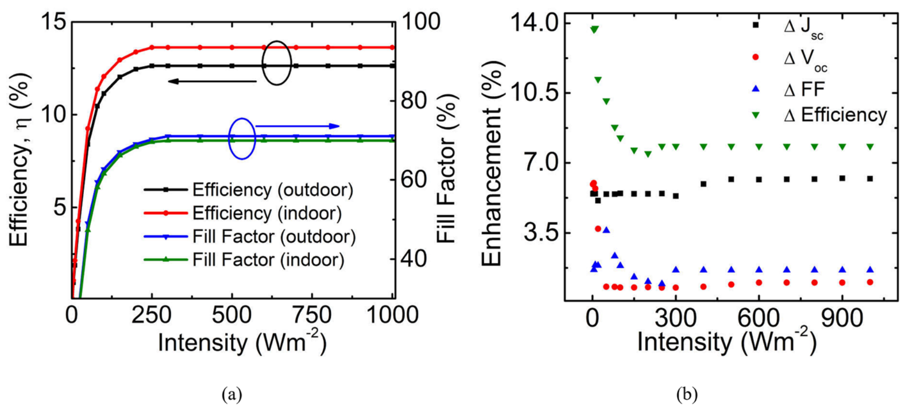

FIG. 2. (a) Efficiency and fill factor as a function of intensity under both indoor and solar illumination conditions in Device A; (b) relative enhancement of short circuit current density (J_{sc}), open circuit voltage (V_{oc}), fill factor (FF) and efficiency (η) with respect to outdoor solar illumination conditions for varying intensities of the indoor light source.

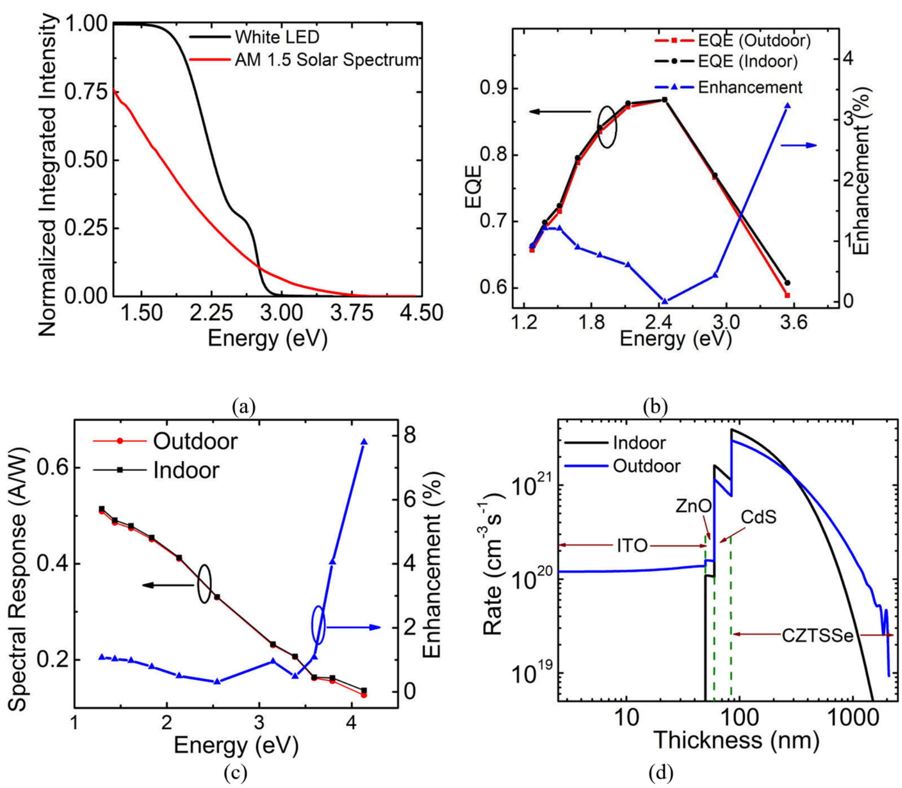

FIG. 3. (a) Normalized integrated intensity as a function of photon energy for white LED and solar spectra; (b) external quantum efficiency (EQE) profiles for indoor and solar illumination conditions in Device A along with the relative enhancement of EQE; (c) spectral response for indoor and solar illumination along with the relative increase of spectral response for indoor illumination with respect to solar illumination condition, (d) generation rates in different regions of Device 1 for both indoor and outdoor conditions.

for the case of indoor illumination. As photo-generation near the junction is dominated by absorption of short-wavelength component of the spectrum, it is likely that the high photon yields at short wavelengths of the LED spectrum results in higher generation rates in the CZTSSe device compared to the rates obtained under solar radiation.

III. PERFORMANCE ENHANCEMENT UNDER INDOOR CONDITION

The results discussed so far indicate that performance enhancement of the CZTSSe device is primarily limited by the marginal enhancement of V_{oc} under indoor condition, even though J_{sc} increases substantially at all intensity levels of the indoor spectra. To further enhance efficiency of the device, we propose a modified heterostructure which is denoted as Device B in Table I. In this structure, the n-doped ZnO and n-ITO layers of Device A are replaced with intrinsic ZnO and n (Al)-doped ZnO respectively. This proposed device can be experimentally fabricated employing low-cost, non-vacuum deposition techniques which have been already utilized for fabricating CZTSSe PV devices.[20] Moreover, Al-doped ZnO is considered to be an effective replacement of ITO as a transparent conductive oxide because of its equivalent performance characteristics at relatively low cost.[21] To elucidate the advantage of

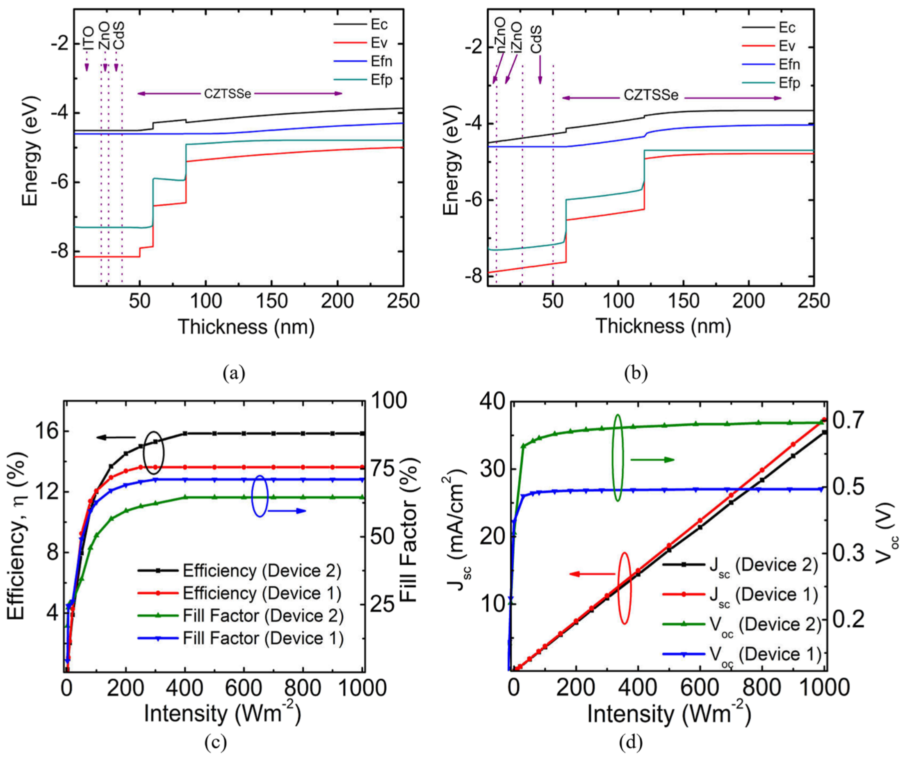

FIG. 4. (a) Band diagram of Device A and (b) Device B under identical indoor illuminations; (c) efficiency, fill factor and (d) J_{sc}, V_{oc} of Device A and Device B for different intensities of the illuminating white LED source.

Device B over Device A, non-equilibrium energy band diagrams of both these devices are compared in Fig. 4(a)–(b). Whereas Device A has a straddling (type I) heterostructure, the energy band of Device B is staggered (type II) in nature because of the conduction band offsets between ZnO and CZTSSe.[22,23] As discussed in Ref. 24, energy spike appearing in the conduction band of straddling gap heterostructure can possibly increase the open circuit voltage of the device. However the intrinsic ZnO layer in Device B results in a built-in field of 6.6×10^8 V/cm, which is approximately 11% higher than the value obtained for Device A. This higher built in field effectively enhances separation of photo-generated carriers near the junction, which is evident from the larger energy difference of quasi Fermi levels (ΔE_f) in Device B than in Device A under identical indoor conditions. Consequently, as illustrated in Figs. 4(c)–(d), Device B exhibits a higher open circuit voltage and overall efficiency than does Device A under indoor illumination of varying intensities. The relatively lower short-circuit current density of Device B is related to the incorporation of n-ZnO layer, which has higher absorption characteristics than that of ITO within 400-800 nm range of the optical spectrum.[25] Moreover, because of the relatively low electron and hole mobilities of the intrinsic ZnO layer, the fill factor of Device B remains lower than that of Device A as shown in Fig. 4(c).[26] In spite of the reduced J_{sc} and FF, open circuit voltage in Device B is ~ 40% higher with respect to the V_{oc} values obtained in Device A, thereby resulting in the higher overall efficiency of Device B. Therefore, for indoor applications, an optimization can be attained in the design of PV devices such that the efficiency can be enhanced by improving the V_{oc}, albeit at the cost of reduced J_{sc} and FF. It is envisaged that further design considerations of indoor PV-devices can be explored by investigating indoor spectra-dependent performance analysis, a study which was beyond the scope of the present work.

IV. CONCLUSION

Performance characteristics of CZTSSe photovoltaic device with respect to indoor energy harvesting applications is investigated using numerical analysis. The study shows that enhancement of efficiency and FF of a CZTSSe photovoltaic device under indoor condition is related to the high photon yield of the illuminating indoor spectrum, which results in higher generation rates, spectral response and subsequently higher open circuit voltage and short circuit current at low and high intensities respectively. Further efficiency enhancement is obtained by designing a type-II heterostructure, in which better charge separation improves the open circuit voltage by 40%. The study shows that in spite of the high photon yield, efficiency enhancement in a CZTSSe device is limited by its external quantum efficiency profile, the peak of which may not coincide with the high photon yield regime corresponding to the indoor spectrum. Hence performance optimization of PV devices under indoor operation requires detailed spectra dependent analysis with due consideration of the heterostructure.

ACKNOWLEDGMENTS

The authors would like to acknowledge the support of the Department of Electrical and Electronic Engineering, Bangladesh University of Engineering and Technology.

SUPPLEMENTARY MATERIAL

See supplementary material for detailed description of the theoretical model and list of material parameters used in this study.

REFERENCES

[1] C. Knight, J. Davidson, and S. Behrens, Sensors **8**, 8037–8066 (2008).
[2] A. S. Teran, E. Moon, W. Lim, G. Kim, I. Lee, D. Blaauw, and J. D. Phillips, IEEE Transactions on Electron Devices **63**, 2820 (2016).
[3] A. S. Teran, J. Wong, W. Lim, G. Kim, Y. Lee, D. Blaauw, and J. D. Phililps, IEEE Transactions on Electron Devices **62**, 2170 (2015).
[4] I. Mathews, P. J. King, F. Stafford, and R. Frizzell, IEEE Journal of Photovoltaics **6**, 230 (2016).
[5] J. Russo, W. Ray, and M. S. Litz, Applied Energy **191**, 10 (2017).
[6] W. Shockley and H. J. Queisser, Journal of Applied Physics **32**, 510 (1961).
[7] M. Freunek, M. Freunek, and L. M. Reindl, IEEE Journal of Photovoltaics **3**, 59 (2013).
[8] J. Randall and J. Jacot, Renewable Energy **28**, 1851 (2003).
[9] J. Manser, J. Christians, and P. Kamat, Chemical Reviews **116**, 12956 (2016).
[10] J. Nelson, Materials Today **14**, 462 (2011).
[11] B. O'Regan and M. Graetzel, Nature **353**, 737 (1991).
[12] C. S. Tao, J. Jiang, and M. Tao, Solar Energy Materials and Solar Cells **95**, 3176 (2011).
[13] S. Das, K. Mandal, and R. N. Bhattacharya, Semiconductor Materials for Solar Photovoltaic Cells **218**, 25 (2016).
[14] M. Green, Y. Hishikawa, E. Dunlop, D. H. Levi, J. Hohl-Ebinger, and A. Ho-Baillie, Progress in Photovoltaics **26**, 3 (2017).
[15] J. Randall, *Designing Indoor Solar Products: Photovoltaic Technologies for AES* (John Wiley & Sons, Ltd, 2006).
[16] M. F. Müller, *Indoor Photovoltaics: Efficiencies, Measurements and Design* (Scrivener Publishing LLC, 2013).
[17] A. Sacco, L. Rolle, L. Scaltrito, E. Tresso, and C. F. Pirri, Applied Energy **102**, 1295 (2013).
[18] W. Wang, M. T. Winkler, O. Gunawan, T. Gokmen, T. K. Todorov, Y. Zhu, and D. B. Mitzi, Advanced Energy Materials **4**, 1301465 (2014).
[19] R. Varache, C. Leendertz, M. Gueunier-Farret, J. Haschke, D. Muñoz, and L. Korte, Solar Energy Materials and Solar Cells **141**, 14 (2015).
[20] S. Bag, O. Gunawan, T. Gokmen, Y. Zhu, T. K. Todorov, and D. B. Mitzi, Energy Environ. Sci. **5**, 7060 (2012).
[21] N. Neves, R. Barros, E. Antunes, J. Calado, E. Fortunato, R. Martins, and I. Ferreira, Journal of the European Ceramic Society **32**, 4381 (2012).
[22] S. Chen, A. Walsh, J.-H. Yang, X. G. Gong, L. Sun, P.-X. Yang, J.-H. Chu, and S.-H. Wei, Phys. Rev. B **83**, 125201 (2011).
[23] A. Walsh, S. Y. Chen, S.-H. Wei, and X. Gong, Advanced Energy Materials **2**, 400 (2012).
[24] K. Ito, *Copper Zinc Tin Sulfide-Based Thin-Film Solar Cells* (John Wiley & Sons, Ltd, 2015).
[25] J. Muth, R. Kolbas, A. Sharma, S. Oktyabrsky, and J. Narayan, Journal of Applied Physics **85**, 7884 (1999).
[26] M. Courel, F. Pulgarin-Agudelo, J. Andrade-Arvizu, and O. Vigil-Galán, Solar Energy Materials and Solar Cells **149**, 204 (2016).